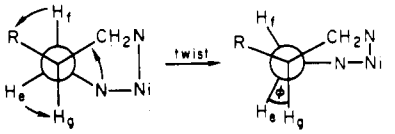

(1)

coupling between H_e and H_g should increase as the dihedral angle between them approaches 0°. In addition, the coupling between H_f and H_g should decrease as a result of the decrease in their dihedral angle from 180 to 120°. When ϕ reaches 30°, the predicted coupling constants, J_{eg} and J_{fg}, would be 6.0 and 6.9 Hz, which are close to the experimentally observed couplings.

We can compare the predicted conformation for the propanediamine ring in complex **7** with a similar copper chelate that has been analyzed by X-ray crystallography. The crystal structure of III [bis(2-hydroxyacetophenone) trimethylenediiminato]copper(II),[28] shows that the six-membered copper-propanediamine ring takes a twisted-boat conformation. If the nickel complex, **7**, were to adopt the same conformation, the dihedral angle, ϕ (see eq 1), between H_e and H_g would be approximately 30°, which is the value obtained from the ^1H NMR results using the Karplus equation. Thus, on going from the fused 6-, 6-, and 6-membered chelate rings in complex **7** to the 5-, 6-, and 5-membered rings in complex **5**, there is a change in the conformation of the central chelate ring, which shows itself by the observed difference in the ^1H NMR spectra of **5** and **7**.

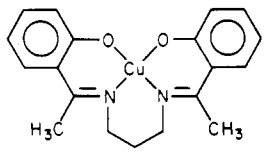

III

(28) Iida, K.; Oonishi, I.; Nakahara, A.; Komiyama, Y. *Bull. Chem. Soc. Jpn.* **1970**, *43*, 2347.

Summary

The physical and spectral properties of the binuclear complexes reported here parallel those of their mononuclear analogues. The visible spectra of the binuclear complexes are nearly identical with those of the corresponding mononuclear complexes. A comparison of the magnetic moments determined in solution of the binuclear complexes with their mononuclear counterparts reveals nearly identical values, suggesting the metal centers in the binuclear complex are sufficiently insulated from one another to prevent significant electronic interactions between them. While conductivity measurements suggest some metal–ligand–metal interactions in the pyridinecarbaldimine complexes, studies are continuing in order to obtain more direct evidence for this type of interaction. The use of high-field NMR has provided conclusive evidence for the binuclear structure of complex **5**. In addition, it has allowed a conformational analysis to be performed for the binuclear nickel complexes through the use of the Karplus relationship.[26] relationship.[26] Further studies of these and related binuclear complexes are in progress.

Acknowledgment. We thank the Office of Naval Research and the National Science Foundation (Grant CHE83-08064) for support of the research. B.C.W. gratefully acknowledges a Sherman Clarke Fellowship.

Registry No. **1**, 70865-15-5; **2a**, 89178-09-6; **2b**, 89178-10-9; **2c**, 89178-11-0; **3**, 89178-12-1; **4**, 89178-13-2; **5**, 89178-14-3; **6**, 89178-15-4; $Co((pya)_2prn)Cl_2$, 89178-16-5; $Ni((pya)_2prn)Cl_2$, 39489-09-3; $Cu((pya)_2prn)Cl_2$, 89178-17-6; $Cu((pyrr)_2prn)$, 16389-93-8; $Ni((pya)_2prn)(N_3)_2$, 39489-05-9; $Ni((pya)_2prn)(SCN)_2$, 39489-04-8; 2-pyridinecarbaldehyde, 1121-60-4; 2-pyrrolecarbaldehyde, 1003-29-8.

Contribution from the Department of Chemistry, University of Houston, Houston, Texas 77004

The Four-Electron Oxidation of a Novel μ-Oxo Dimer, $[((p\text{-}Et_2N)TPP)Fe]_2O$

D. CHANG, P. COCOLIOS, Y. T. WU, and K. M. KADISH*

Received September 19, 1983

The oxidation of $[((p\text{-}Et_2N)TPP)Fe]_2O$ (**1**) and $((TPP)Fe)_2O$ (**2**) was investigated in CH_2Cl_2 by electrochemical and spectral techniques. Contrary to expectation, four, and not three, electrons were abstracted from each dimer. The first electron transfer (at 0.34 V vs. SCE for **1** and 0.84 V vs. SCE for **2**) involved formation of a cation radical delocalized on both of the porphyrin rings. The most anodic two-electron oxidation of **1** (at 0.76 V) was consistent with a reaction involving oxidation of two noninteracting equivalent reaction sites. This is the first example of such a reaction with iron porphyrins. A similar two-electron oxidation was also observed for **2**, but in this case, the reaction sites appear to be interacting and the half-wave potentials were separated by 90 mV. The one- and two-electron-oxidized complexes of **1** were chemically generated and isolated in the solid state as the mono- and diperchlorate salts. ^1H NMR and IR spectroscopic methods were used to identify the initial reactants while IR, ESR, and electronic absorption spectroscopy and rotating-disk voltammetry were used to characterize the oxidation products of each electron-transfer step.

Introduction

The electrochemical and chemical oxidation of $((TPP)Fe)_2O$ has been reported in nonaqueous media.[1-5] Both the singly and doubly oxidized complexes have been isolated,[5] and after a great deal of controversy,[6] there is now little doubt that initial electron abstraction involves orbitals of the porphyrin ring to

(1) Felton, R. H.; Owen, G. S.; Dolphin, D.; Forman, A.; Borg, D. C.; Fajer, J. *Ann. N.Y. Acad. Sci.* **1973**, *206*, 504.
(2) Kadish, K. M.; Cheng, J. S.; Cohen, I. A.; Summerville, D. *ACS Symp. Ser.* **1977**, *No. 38*, 65.
(3) Phillippi, M. A.; Goff, H. M. *J. Am. Chem. Soc.* **1979**, *101*, 7641.
(4) Phillippi, M. A.; Shimomura, E. T.; Goff, H. M. *Inorg. Chem.* **1981**, *20*, 1322.
(5) Phillippi, M. A.; Goff, H. M. *J. Am. Chem. Soc.* **1982**, *104*, 6026.
(6) Reed, C. A. In "Electrochemical and Spectrochemical Studies of Biological Redox Components"; Kadish, K. M., Ed.; American Chemical Society: Washington, DC, 1982; Adv. Chem. Ser. No. 201, p 333.

0020-1669/84/1323-1629$01.50/0

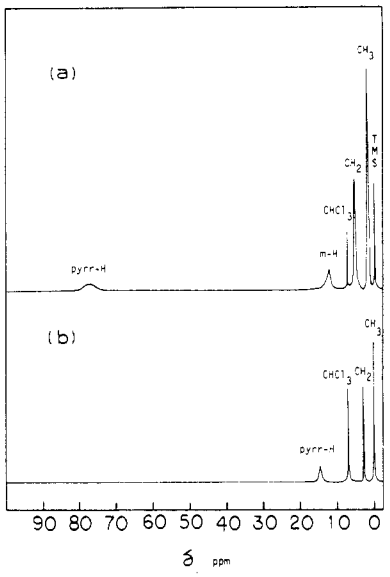

Figure 1. ^1H NMR spectra ($CDCl_3$, 294 K): (a) ((*p*-Et_2N)TPP)FeCl; (b) [((*p*-Et_2N)TPP)Fe]$_2O$.

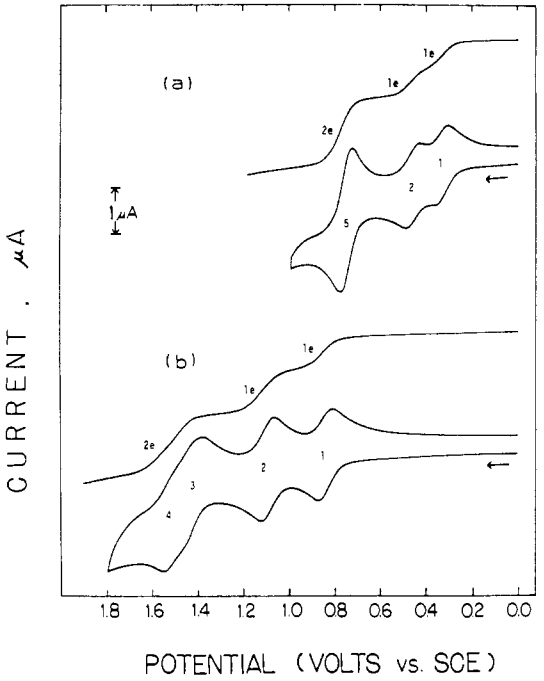

Figure 2. Rotating-disk voltammograms (rotation speed 500 rpm, scan rate 0.005 V/s) and cyclic voltammograms at a Pt electrode (scan rate 0.1 V/s) recorded in CH_2Cl_2/0.1 M TBAP: (a) [((*p*-Et_2N)TPP)Fe]$_2O$; (b) ((TPP)Fe)$_2O$. The numbers 1–5 are identified in Scheme I.

form cation π radicals and dications. Further oxidations are also possible for iron tetraphenylporphyrin dimers, and a third oxidation has been reported in the range of +1.33 to +1.46 V vs. SCE.[2,4]

In a recent publication it was shown that ruthenium(II) tetraphenylporphyrin oxidation potentials could be shifted toward negative values by 550–600 mV through the introduction of diethylamino substituents on the four phenyl rings.[7] We now report the oxidation potentials and product characterization of an iron porphyrin dimer containing these same electron-donating substituents. By use of these highly electron-donating substituents on the investigated complex [((*p*-Et_2N)TPP)Fe]$_2O$ (**1**), we were able to produce porphyrin radical cations and dications at less positive potentials than had ever been observed before. The singly and doubly oxidized complexes of **1** were stable enough to be isolated and characterized in the solid state. At the same time we were able to easily characterize the more highly oxidized forms of the iron porphyrins since their oxidation potentials do not overlap with the potential limit of CH_2Cl_2 (+1.7 V vs. SCE).

Experimental Section

Instrumentation. ^1H NMR spectra were recorded on a Varian XL-100 spectrometer. Spectra were measured of solutions of 10 mg of sample in 0.5 mL of $CDCl_3$ with tetramethylsilane as internal reference. IR spectra were performed on a Perkin-Elmer 1330 spectrophotometer. Samples were 1% dispersions in CsI pellets. Cyclic voltammetric measurements were made by using a conventional three-electrode configuration and a combination of a Princeton Applied Research (PAR) Model 174A polarographic analyzer/Model 175 universal programmer. A platinum button served as a working electrode and a platinum wire as a counterelectrode. A saturated calomel electrode (SCE), which was separated from the bulk of the solution by a fritted-glass disk, was used as the reference electrode. Current–voltage curves were recorded on a Houston Instruments Omnigraphic X-Y recorder.

Bulk-scale coulometry and controlled-potential electrolysis were done by using a PAR Model 173 potentiostat to control the potential. Integration of the current–time curve was achieved by means of a PAR Model 179 integrator. A three-electrode configuration was used, consisting of a Pt-wire-mesh working electrode, a Pt-wire counterelectrode separated from the main solution by a glass frit, and an SCE as the reference electrode. Deaeration and stirring were achieved by means of a stream of high-purity nitrogen, which was passed throughout the solution.

Spectroelectrochemistry was performed in a bulk cell, which followed the design of Fajer et al.[8] and had an optical path length of 0.19 cm. The SCE was separated from the test solution by a fritted bridge containing solvent and supporting electrolyte. A Tracor Northern 1710 optical spectrometer/multichannel analyzer was used to obtain time-resolved spectra. Each acquisition represents a single spectrum from 290 to 917 nm simultaneously recorded by a double-array detector with a resolution of 1.2 nm/channel.

ESR spectra were recorded on an IBM Model ER 100D spectrometer equipped with a microwave bridge ER 040-X and an ER 080 power supply. Low-temperature ESR spectral measurements were achieved with a Varian variable-temperature controller that monitored the temperature from 273 to 123 K. For 77 K measurements, samples were introduced into the cavity in a sealed quartz tube immersed in a liquid-nitrogen Dewar. The *g* values were measured relative to diphenylpicrylhydrazyl (DPPH) (g = 2.0036 ± 0.0003).

Chemicals. Unless otherwise noted, all reagents were obtained from commercial suppliers and used without further purification. Technical grade methylene chloride, CH_2Cl_2, was twice distilled from P_2O_5 prior to use. The supporting electrolyte, tetrabutylammonium perchlorate (TBAP) (Eastman Chemicals), was recrystallized from ethyl acetate/*n*-hexane and dried in vacuo.

Free-base (*p*-Et_2N)TPPH_2 was prepared according to literature procedures[9] by using 4-(diethylamino)benzaldehyde (Alfa Chemicals) and pyrrole (Aldrich). Insertion of iron into the porphyrin core was performed with $FeCl_2 \cdot 4H_2O$ in DMF[10] or pyridine and gave similar results. The obtained product was entirely converted to the dimer **1** either by elution with chloroform over a basic alumina column or by basic hydrolysis using a 2 M aqueous NaOH solution. The chemical oxidation of [((*p*-Et_2N)TPP)Fe]$_2O$ (**1**) was performed by adding 1 or 2 equiv of $I_2/AgClO_4$ to a solution of **1** in methylene chloride.[11] The obtained mono- and dication were isolated as the mono- and diperchlorate salts. Typical experiments are described below.

[((*p*-Et_2N)TPP)Fe]$_2O$. A 550-mg (0.56 mmol) sample of (*p*-Et_2N)TPPH_2 in 50 mL of pyridine was added to a 25-mL refluxing

(7) Malinski, T.; Chang, D.; Bottomley, L. A.; Kadish, K. M. *Inorg. Chem.* **1982**, *21*, 12, 4248.

(8) Fajer, J.; Borg, D. C.; Forman, A.; Dolphin, D.; Felton, R. H. *J. Am. Chem. Soc.* **1970**, *92*, 3451.

(9) Datta-Gupta, N.; Bardos, T. J. *J. Heterocycl. Chem.* **1966**, *3*, 495.

(10) Walker, F. A.; Balke, V. L.; McDermott, G. A. *J. Am. Chem. Soc.* **1982**, *104*, 1569.

(11) Shine, H. J.; Padilla, A. G.; Wu, S. M. *J. Org. Chem.* **1979**, *44*, 4069.

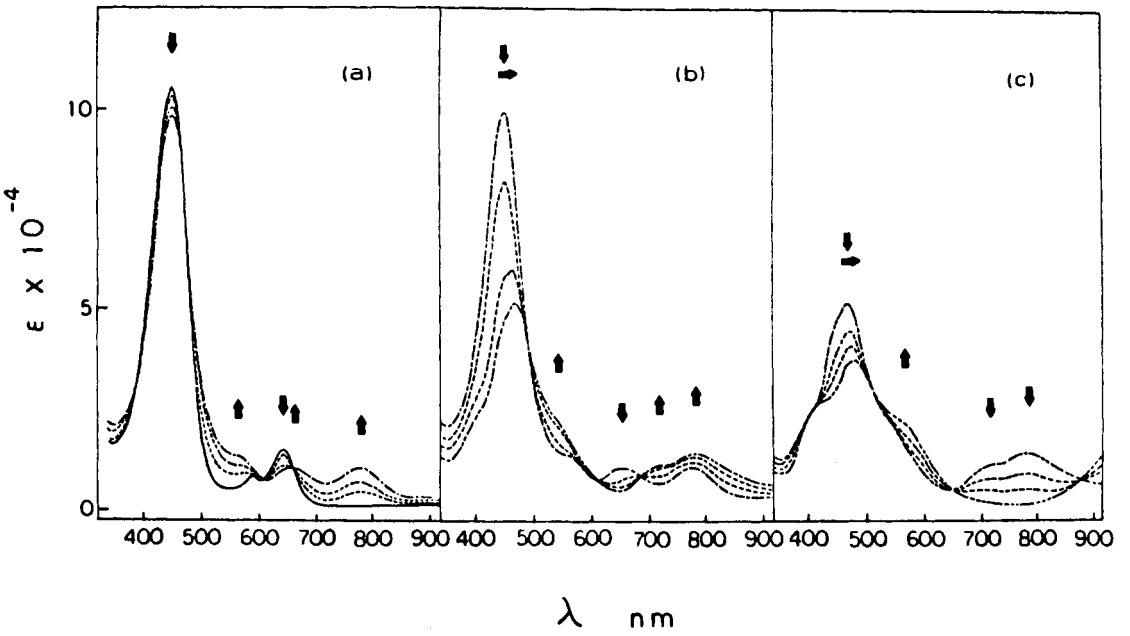

Figure 3. Time-resolved electronic absorption spectra of $[((p\text{-}Et_2N)TPP)Fe]_2O$ obtained during controlled-potential oxidation in CH_2Cl_2/0.1 M TBAP: (a) before oxidation (—) and at E_{app} = 0.4 V; (b) at E_{app} = 0.6 V; (c) at E_{app} = 0.9 V.

solution of pyridine containing 550 mg (2.78 mmol) of $FeCl_2 \cdot 4H_2O$, and the mixture was heated for 1 h. After cooling, 100 mL of toluene was added and the solvent evaporated on a rotavap under vacuum. The crude material was then dissolved in CH_2Cl_2, and the unreacted inorganic salts were removed by suction filtration. The solution was twice shaken with a 2 M aqueous NaOH aliquot, washed with water until neutrality, and dried over magnesium sulfate. The chromatographic purification of compound **1** was achieved on a basic alumina column eluated with a 98/2 mixture of methylene chloride/acetone. After concentration of the solution and addition of *n*-hexane, 450 mg (84%) of pure dimer was collected. ^1H NMR ($CDCl_3$, 21 °C): δ_{pyrr} = 13.4, δ_{phenyl} = 7.3 (br), δ_{CH_2} = 3.65, δ_{CH_3} = 1.45. IR: $\nu_{Fe\text{-}O\text{-}Fe}$ = 900, 885 cm^{-1}.

((p-Et2N)TPP)FeCl. A 100-mg (0.052 mmol) sample of pure dimer **1** in 40 mL of CH_2Cl_2 was converted to $[((p\text{-}Et_2N^+H)TPP)FeCl](Cl^-)_4$ by bubbling anhydrous HCl through the solution. After evaporation of the solvent under reduced pressure, 400 mg (0.208 mmol) of **1** in 160 mL of CH_2Cl_2 was added and the mixture was heated under reflux for 15 min. After removal of the solvent and recrystallization of the crude solid in toluene/*n*-heptane, 410 mg (80%) of ((*p*-Et_2N)TPP)FeCl was obtained. ^1H NMR ($CDCl_3$, 21 °C): δ_{pyrr} = 78.3, $\delta_{m\text{-}H}$ = 12.4, δ_{CH_2} = 5.41, δ_{CH_3} = 1.91. IR: $\nu_{Fe\text{-}Cl}$ = 355 cm^{-1}.

$[((p\text{-}Et_2N)TPP)Fe]_2O^+ClO_4^-$. A 7.7-mg (0.030 mmol) sample of iodine in 1 mL of CH_2Cl_2 and 12.5 mg (0.060 mmol) of silver perchlorate in 0.5 mL of acetonitrile were added to 100 mg (0.052 mmol) of **1** in 10 mL of CH_2Cl_2. After filtration from AgI, the $[((p\text{-}Et_2N)TPP)Fe]_2O^+ClO_4^-$ salt was precipitated by *n*-hexane to give 75 mg (71%). IR: $\nu_{ClO_4^-}$ = 1100, 622 cm^{-1}.

$[((p\text{-}Et_2N)TPP)Fe]_2O^{2+}(ClO_4^-)_2$. A 2-equiv portion of $I_2/AgClO_4$ was added to a 100-mg solution of **1** as described above, and 83 mg (75%) of the doubly oxidized complex was produced. IR: $\nu_{ClO_4^-}$ = 1125, 1100, 622 cm^{-1}.

Results and Discussion

Figure 1 shows the ^1H NMR spectra of complex **1** and its precursor. For ((*p*-Et_2N)TPP)FeCl the resonance signal of the pyrrolic protons at δ 78.3 downfield from internal Me_4Si suggests a pentacoordinate high-spin $S = {}^5/_2$ species.[12] The resonance signal of the meta phenyl protons is a singlet at δ 12.4.[13] This unusual resonance for such complexes might be attributed to an increased rate of phenyl-ring rotation, which is due to the presence of the electron-donating Et_2N groups at the para position.[13] For compound **1** the oxygen bridge leads to an antiferromagnetically coupled iron dimer with δ_{pyrr} = 13.4. The IR spectra of these two compounds also exhibit characteristic stretching frequencies at 355 ($\nu_{Fe\text{-}Cl}$) and at 900 and 885 cm^{-1} ($\nu_{Fe\text{-}O\text{-}Fe}$).

Both cyclic voltammetry and rotating-disk voltammetry of **1** at a Pt electrode in CH_2Cl_2 are shown in Figure 2a and indicate three diffusion-controlled oxidations (at $E_{1/2}$ = 0.34, 0.47, and 0.76 V), with the currents for the latter oxidation suggesting a two-electron abstraction. The anodic to cathodic peak separation of all three oxidations by cyclic voltammetry is 60 ± 5 mV at low scan rates and $i_p/v^{1/2}$ is constant, suggesting the absence of chemical reactions coupled to the electron transfers. This 60-mV separation for the latter oxidation might be interpreted as a one-electron transfer, but as will be shown later, this process involves the overall two-electron oxidation of two noninteracting equivalent reaction sites. A further, multiple-electron abstraction (which is coupled with adsorption of the product and blocking of the electrode surface) is also observed at 1.20 V. This reaction most likely involves oxidation of the Et_2N substituents and is not the subject of this study, which concentrates only on the initial four-electron oxidation of each complex.

Coulometric measurements were made at potentials anodic of each peak and are consistent with the reversible abstraction of one, one, and two electrons for each of the three peaks. The 77 K ESR spectrum observed after oxidation of **1** at an applied potential of 0.40 V had a signal at g = 1.997 and gave the electronic absorption spectrum shown in Figure 3a. Both the g values and the peak at λ = 777 nm are consistent with formation of a cation radical.[8,14,15] Further electrolysis at 0.60 V showed the disappearance of this ESR signal and gave the radical type spectrum shown in Figure 3b. Finally, the overall two-electron oxidation at 0.76 V gave the absorption spectrum shown in Figure 3c.

Infrared spectra for the neutral complex as well as the higher oxidized forms of **1** are shown in Figure 4. As expected, the singly and doubly oxidized complexes exhibit characteristic

(12) Lamar, G. N.; Walker, F. A. In "The Porphyrins"; Dolphin, D., Ed.; Academic Press: New York, 1979; Vol. IV, p 93.
(13) Eaton, S. S.; Fishwild, D. M.; Eaton, G. R. *Inorg. Chem.* **1978**, *17*, 1542.
(14) Wolberg, A.; Manassen, J. *J. Am. Chem. Soc.* **1970**, *92*, 2982.
(15) We observed a similar peak at λ = 777 nm for $[((p\text{-}Et_2N)TPP)Cu]^+$ and for $[((p\text{-}Et_2N)TPP)Zn]^+$ in CH_2Cl_2/0.1 M TBAP.

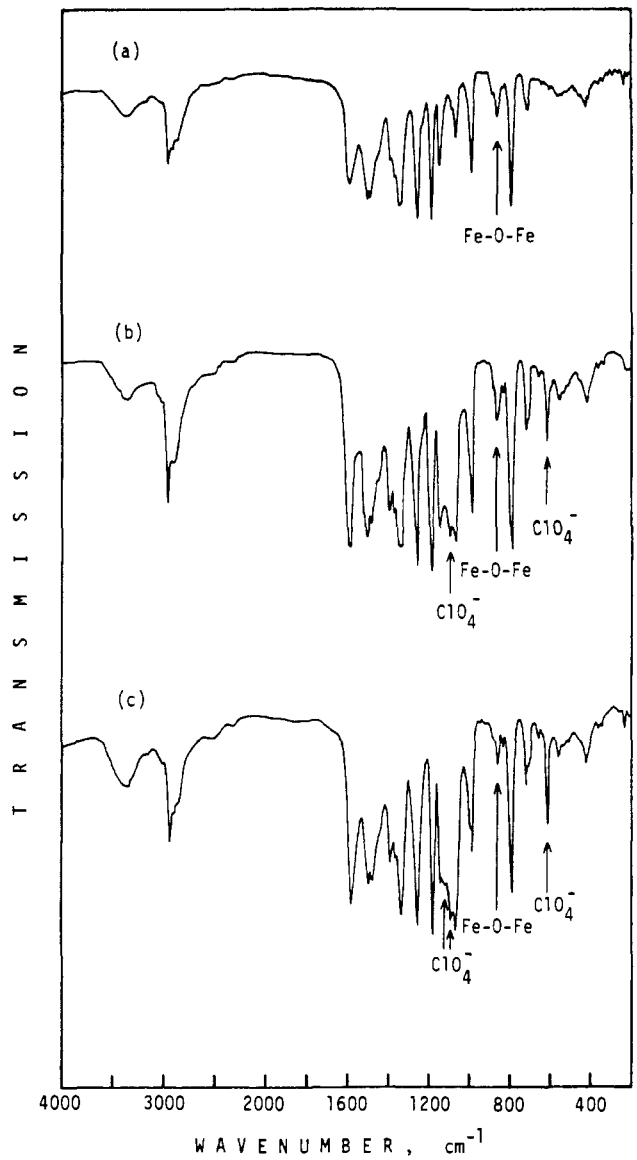

Figure 4. IR spectra (CsI pellets): (a) $[((p\text{-}Et_2N)TPP)Fe]_2O$ (**1**); (b) $[((p\text{-}Et_2N)TPP)Fe]_2O^+ClO_4^-$; (c) $[((p\text{-}Et_2N)TPP)Fe]_2O^{2+}(ClO_4^-)_2$.

stretching frequencies for the ClO_4^- group at 1100 and 622 cm^{-1} and at 1125, 1100, and 622 cm^{-1}, respectively. Their spectra display characteristic Fe–O–Fe stretching frequencies at 885 cm^{-1}, suggesting that both oxidized complexes are in the dimeric form. Also, their electronic absorption spectra in CH_2Cl_2 and the solid-state ESR of singly oxidized **1** (5% in a powder magnesium sulfate matrix) are identical with those obtained by electrochemical oxidation of **1**. Finally, identically shaped rotating-disk voltammograms were obtained for the neutral, the singly oxidized, and the doubly oxidized complexes of **1**, but in the later two cases, the zero current was displaced as expected for compounds that undergo both oxidation and reduction.

An overall four-electron oxidation also occurs for $((TPP)Fe)_2O$ (**2**). Figure 2b illustrates a cyclic voltammogram of **2** at a Pt electrode in CH_2Cl_2/0.1 M TBAP. All of the peaks are diffusion controlled, and the shape of the curve is similar, but not identical, to that reported in the literature.[2] The significant difference from previous results is that the most positive peak (reported at +1.45 V[2,4]) actually consists of two overlapping processes ($E_{1/2}$ = 1.41, 1.52 V).[16] This is also evident by differential-pulse polarography, which has peaks at E_p = 1.45 and 1.50 V (at a modulation amplitude of 5 mV)

Scheme I

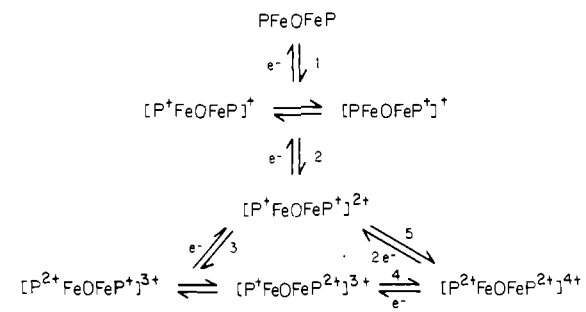

and by rotating-disk voltammetry (Figure 2b), which clearly shows a height consistent with two electrons transferred in the process near +1.45 V. The shape of the current–voltage curve is consistent with an EE mechanism where the second oxidation is shifted from the first by approximately 90 mV.[17]

Analysis of these electrochemical data, as well as the electronic absorption spectra and ESR of the oxidized products, suggests that the overall initial four-electron oxidation of both **1** and **2** may be described by Scheme I, where P = TPP or $(p\text{-}Et_2N)TPP$ and 1–5 represent the electron-transfer steps shown in Figure 1.

According to Scheme I, oxidation of the second porphyrin ring on the dimer (reaction 2) is more difficult than oxidation of the first (reaction 1). This difference is due to electrostatic interactions between the two sites and amounts to 250 mV for **2** but only 140 mV for **1**. Formation of the dication of **2** also involves separate processes, at 1.41 V (reaction 3) and 1.52 V (reaction 4). This difference in potential does not exist for dication formation of **1**, and both oxidations occur at an identical potential of 0.76 V (reaction 5).

The theory for electron transfer from molecules containing multiple noninteracting redox centers has been described in the literature[18] and appears to fit this last reaction exactly. The coulometric value of n = 2, the height of the diffusion current by rotating-disk voltammetry, and the Nernstian peak separation of 60 mV clearly suggest that there is no interaction across the oxo bridge of $[P^+FeOFeP^+]^{2+}$. This is not the case for the uncharged PFeOFeP complex, which appears to have strong interaction between the two reaction sites, thus producing separate half-wave potentials for radical cation formation.

In summary, we have shown that ferric porphyrin dimers may be oxidized by four electrons to yield stable, highly charged complexes. We have also shown that radical cations of porphyrin dimers may be significantly shifted in potential by the use of electron-donating substituents so that, in the case of **1**, the initial oxidation occurs at 0.34 V. This is the most negative cation radical ever reported for a ferric porphyrin dimer. Finally, we have shown the first two-electron oxidation of a metalloporphyrin system where the electron is abstracted from two equivalent noninteracting reaction sites. This suggests the possibility of multiple electron abstraction at a given potential using a properly designed polymeric metalloporphyrin system.

Acknowledgment. The support of the National Institutes of Health (Grant GM 25172) is gratefully acknowledged.

(16) Reexamination of Figure 2b in ref 2 shows that the third oxidation peak of $((TPP)Fe)_2O$ has a peak current larger than the first two oxidations and a shape indicative of closely overlapping processes. The appearance of separate peaks in this study is most likely due to differences in the electrode surface properties or possibly to small differences in the solvent/supporting electrolyte mixture that would lead to differences in solution between the two studies.

(17) Polcyn, D. S.; Shain, I. *Anal. Chem.* **1966**, *38*, 370.
(18) Flanagan, J. B.; Margel, S.; Bard, A. J.; Anson, F. C. *J. Am. Chem. Soc.* **1978**, *100*, 4248.

Registry No. **1**, 89177-90-2; 1^{2+}, 89345-75-5; **2**, 12582-61-5; 2^{2+}, 72319-57-4; ((*p*-Et_2N)TPP)FeCl, 85529-39-1; [((*p*-Et_2N)TPP)-$Fe]_2O^+ClO_4^-$, 89177-92-4; [((*p*-Et_2N)TPP)$Fe]_2O^{2+}(ClO_4^-)_2$, 89363-51-9.

Notes

Contribution from the Department of Macromolecular Science, Osaka University, Toyonaka, Osaka, 560 Japan, and Department of Chemistry, Cornell University, Ithaca, New York 14853

σ vs. π Bonding in Organoactinides and Possibilities of CO Coordination to Actinides

Kazuyuki Tatsumi† and Roald Hoffmann*‡

Received September 30, 1983

To find similarity or to search for differences, the antithetical and yet complementary lines of approach to science, are the ways in which organoactinide chemistry has been fostered, being weighed against d-block transition-metal chemistry.[1] Our extended Hückel analysis of the nature of actinide-to-carbon bonds follows the dual approach. In this communication, we concentrate our attention on the coordination of σ-methyl and π-cyclopentadienyl groups to iron and uranium. The study will then lead us to think that there is nothing wrong with a carbonyl ligand in actinide complexes.

Let us first examine the interaction between Cp and the naked Fe or U atoms, which will reveal the essence of M–Cp bonds.[2] We focus our discussion on $3d^64s^04p^0$ Fe(II) and $5f^06d^07s^07p^0$ U(VI) electron counts, so the charges on the hypothetical molecules are set to be 1+ for FeCp and 5+ for UCp. Figure 1 shows potential energy curves and changes in overlap populations as a function of the M–Cp separation, *L* or *R*. The potential curve for $FeCp^+$ finds a minimum at *R* = 1.92 Å, while a shallow minimum appears at *R* = 2.83 Å in the UCp^{5+} curve. These are fortuitously close to the experimentally observed distances of 2.0–2.1 Å (Fe)[3] and 2.7–2.8 Å (U)[4] in the actual complexes. Although we should not rely on the calculated energies too much because of the approximate nature of the calculations, the good agreement encourages our qualitative analysis.

The intriguing aspect of Figure 1 is the very small U–Cp overlap population. The largest value attained is merely 0.07 at around *R* = 3.2 Å. In the region of the observed U–Cp bond distances, it becomes nearly zero. This contrasts with the large positive overlap populations obtained for $FeCp^+$. The $FeCp^+$ curve shows that the maximum amounts to 0.69 at *R* = 2.0 Å. About 90% of the overlap population comes from the interactions of Cp e_1'' with Fe $3d_{xz}$ (**1**) and $3d_{yz}$ (**2**). For UCp^{5+}, the e_1''–$5f_{xz^2}$ and e_1''–$5f_{yz^2}$ interactions **3** and **4** are available in addition to **1** and **2**, but neither of them is great.

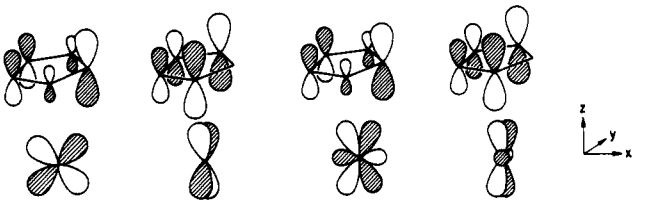

1 **2** **3** **4**

A similar calculation for d^8 $FeCH_3^-$ and f^0d^0 UCH_3^{5+} gives Figure 2. The $FeCH_3^-$ potential energy curve reproduces well the observed distances of 2.0–2.1 Å,[5] while the optimized U–CH_3 distance is at the longer limit of the broad range of observed U–R single bond distances, 2.4–2.7 Å.[6] The Fe–CH_3^- overlap populations are again notable, but more striking, in view of the MCp results, are the fairly large overlap populations calculated for U–CH_3^{5+}. Fe $3d_{z^2}$, 4s, and $4p_z$ all contribute to the Fe–CH_3 σ bond, and for UCH_3^{5+}, $5f_{z^3}$ (**5**) participates in the σ bond as well.

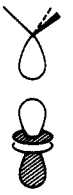

5

The interesting overlap population trends are not artifacts of the analysis based on the naked-metal models. They persist as well in calculations for more realistic molecules, CpFe-$(CO)_2CH_3$ and $Cp_3UCH_3^{2+}$,[7] as displayed in **6** and **7**.

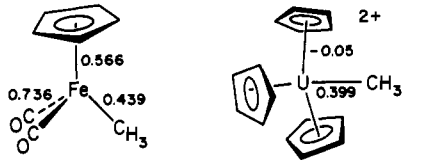

6 **7**

How do the results of the overlap population analysis reflect characteristics of actinide chemistry? The argument runs as follows. The root of the observed trends can be looked for in the nature of M–Cp and M–CH_3 bonds. From the small U–Cp overlap populations, one may deduce that the π bond carries very weak covalent character, if any, while covalency

† Osaka University.

‡ Cornell University.

(1) (a) Marks, T. J. *Science* (*Washington, D.C.*) **1982**, *217*, 989–997 and references therein. (b) Fagan, P. J.; Manriquez, J. M.; Marks, T. J.; Day, C. S.; Vollmer, S. H.; Day, V. W. *Organometallics*, **1982**, *1*, 170.

(2) Atomic parameters are as follows. H_{ii}: Fe, 4s, −8.39 eV; Fe 4p, −4.74 eV; Fe 3d, −11.46 eV. Orbital exponents: Fe 4s, 1.9; Fe 4p, 1.9; Fe 3d, 5.35 (0.5366) + 1.8 (0.6678). The U parameters are taken from: Tatsumi, K.; Hoffmann, R. *Inorg. Chem.* **1980**, *19*, 2656–2658.

(3) For example: (a) Krüger, C.; Barnett, B. L.; Brauer, D. In "The Organic Chemistry of Iron"; Koerner v. Gustorf, E. A., Grevels, F.-W., Fischler, I., Eds.; Academic Press: New York, 1978; pp 1–112 and references therein. (b) Seiler, P.; Dunitz, J. D. *Acta Crystallogr., Sect. B* **1979**, *B35*, 1068–1074.

(4) Raymond, K. N.; Eigerbrot, C. W., Jr. *Acc. Chem. Res.* **1980**, *13*, 276–283 and references therein.

(5) (a) Reference 3. (b) Goedken, V. L.; Peng, S.-M. *J. Am. Chem. Soc.* **1974**, *96*, 7826–7827.

(6) (a) Cramer, R. E.; Higa, K. T.; Pruskin, S. L.; Gilje, J. W. *Organometallics* **1982**, *1*, 869 and references therein. (b) For U–C bonds with multiple bond character, the distances are shorter, ranging from 2.29 to 2.36 Å: Atwood, J. L.; Hains, C. F., Jr.; Tsutsui, M.; Gebala, A. E. *J. Chem. Soc., Chem. Commun.* **1973**, 452–453. Atwood, J. L.; Tsutsui, M.; Ely, N.; Gebala, A. E. *J. Coord. Chem.* **1976**, *5*, 209–215. Cramer, R. E.; Maynard, R. B.; Paw, J. C.; Gilje, J. W. *J. Am. Chem. Soc.* **1981**, *103*, 3589–3590. (c) The longest U–C σ-bond distance was observed in $CpU[(CH_2)_2PPh_2]_3$: Cramer, R. E.; Maynard, R. B.; Gilje, J. W.; Tatsumi, K.; Nakamura, A., to be submitted for publication.

(7) The assumed geometries are as follows: Fe–C(Cp), 2.0 Å; Fe–C(CH_3) and Fe–C(CO), 2.0 Å; U–C(Cp), 2.81 Å, U–C(CH_3), 2.4 Å.

0020-1669/84/1323-1633$01.50/0